

EIGHTY NEW INVARIANTS IN THE ELLIPTIC BILLIARD

DAN REZNIK, RONALDO GARCIA, AND JAIR KOILLER

ABSTRACT. We introduce several-dozen experimentally-found invariants of Poncelet N -periodics in the confocal ellipse pair (Elliptic Billiard). Recall this family is fully defined by two integrals of motion (linear and angular momentum), so any “new” invariants are dependent upon them. Nevertheless, proving them may require sophisticated methods. We reference some two-dozen proofs already contributed. We hope this article will motivate contributions for those still lacking proof.

Keywords: elliptic billiard, invariant, optimization, experimental.

MSC 51N20, 51M04, 65-05

1. INTRODUCTION

The Elliptic Billiard (EB) is a special case of Poncelet’s Porism [13], where the conic pair are two confocal ellipses; it therefore admits a 1d family of N -periodic trajectories [34, 18, 12] which at every vertex are bisected by the normals of the outer ellipse in the pair (hence the term “billiard”); see Figure 1.

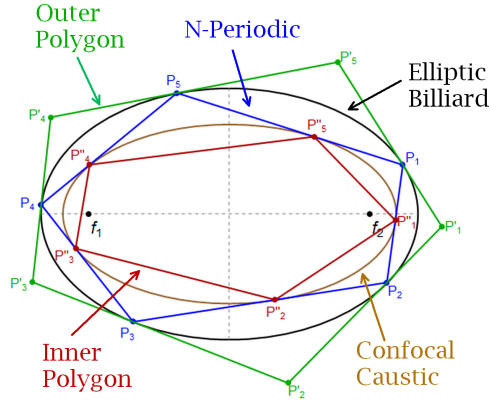


FIGURE 1. A (i) 5-periodic (vertices P_i) is shown inscribed in a confocal ellipse pair (billiard and caustic). Also shown is (ii) the outer polygon with vertices P'_i tangent to the outer ellipse at the N -periodic vertices, and (iii) the inner polygon whose vertices P''_i are at the points of contact of the N -periodic with the caustic.

The EB is an *integrable* system (in fact it is conjectured as the only integrable planar billiard [19]). Integrability implies invariant perimeter L ; a second classic

invariant is Joachimsthal's constant J , which is simply a statement that all trajectory segments are tangent to the confocal caustic [34, 28].

Continuing our work on properties of N -periodics in the EB [26, 16], here we introduce dozens of new invariants detected experimentally. These involve distances, areas, angles and centers of mass of N -periodics and several derived polygons defined below. Some invariants depend on the parity of N , while others on positional constraints.

Note that since the N -periodics in the EB are fully defined by L, J , any “new” invariants listed here or elsewhere must be ultimately dependent upon said quantities. Nevertheless, proving a specific functional dependence may require sophisticated techniques. Several proofs have already been contributed and are referenced below. We hope to motivate more contributions and/or new discoveries.

Admittedly, the number of possible invariants is infinite as one may select any functional combination of L, J . Our selection criterion can be loosely defined as *any quantity constant over the N -periodic family and/or derived objects, which is an elementary function of lengths, angles, areas, etc.*

This article is organized as follows: preliminary definitions are given in Section 2. Invariants are introduced in Section 3, in several clusters, involving: (i) lengths, areas, and angles of N -periodics and associated polygons; (ii) pedal polygons to N -periodics and (iii) their outer polygons; (iv) antipedal polygons (defined below); (v) area-ratios related to the Steiner curvature centroid [33]; (vi) pairs of pedal polygons; (vii) area-ratios of evolute polygons [8]; (viii) focus-inversive objects and (ix) pairs of focus-inversive objects.

Details about our experimental toolbox are covered in Section 4. All symbols used in this article are listed on Table 12 in Appendix A.

We encourage the reader to watch the videos included in Section 5 which provide more insight into invariant phenomena.

Related Work. In a companion article [15] we derive explicit expressions for some of the invariants listed herein for certain “low” N , e.g., 3–6. Methods for obtaining N -periodic trajectories based on Cayley's condition are surveyed in [14, 10]. A few explicit expressions for the caustic parameter (for $N = 3, 4, 6, 8$) appear in [23].

2. PRELIMINARIES

Let the EB have center O , semi-axes $a > b > 0$, and foci f_1, f_2 at $[\pm\sqrt{a^2 - b^2}, 0]$. Let a'', b'' denote the major, minor semi-axes of the confocal caustic, whose values are given by a method due to Cayley [12], though we obtain them numerically, see Section 4.

As mentioned above, the perimeter L is invariant for a given N -periodic family, as is Joachimsthal's constant $J = \langle \mathcal{A}x, v \rangle$, where x is a bounce point (called P_i above), v is the unit velocity vector $(P_i - P_{i-1})/||\cdot||$, $\langle \cdot \rangle$ stands for dot product, and [34]:

$$\mathcal{A} = \text{diag} [1/a^2, 1/b^2]$$

Hellmuth Stachel derived [31] an elegant expression for Joachimsthal's constant J in terms of the axes of the EB and its caustic:

$$J = \frac{\sqrt{a^2 - a''^2}}{ab}$$

Note: holding a constant, for each N , a'' and therefore J assume a distinct value.

Let a polygon have vertices $W_i, i = 1, \dots, N$. In this paper all polygon areas are *signed*, i.e., obtained from a sum of cross-products [22]:

$$(1) \quad S = \frac{1}{2} \sum_{i=1}^N W_i \times W_{i+1}$$

Let $W_i = (x_i, y_i)$, then $W_i \times W_{i+1} = (x_i y_{i+1} - x_{i+1} y_i)$.

The area centroid \overline{W} of a polygon is given by [22]:

$$(2) \quad \overline{W} = \frac{1}{6S} \sum_{i=1}^N (W_i \times W_{i+1})(W_i + W_{i+1})$$

The curvature κ of the ellipse at point (x, y) at distance d_1, d_2 to the foci is given by [35, Ellipse]:

$$(3) \quad \kappa = \frac{1}{a^2 b^2} \left(\frac{x^2}{a^4} + \frac{y^2}{b^4} \right)^{-3/2} = ab(d_1 d_2)^{-3/2} = (\kappa_a d_1 d_2)^{-3/2}$$

Where $\kappa_a = (ab)^{-2/3}$ is the constant affine curvature of the ellipse [21].

Given a polygon with vertices W_i and angles θ_i , its Steiner Centroid of Curvature¹ K is given by [33, p. 22]:

$$(4) \quad K = \frac{\sum_{i=1}^N \rho_i R_i}{\sum \rho_i}, \quad \text{with } \rho_i = \sin(2\theta_i)$$

3. INVARIANTS

In this section we present the invariants found so far in several tables. Each invariant is given an identifier k_n where the first digit of n refers to a cluster of invariants; see Table 1.

¹J. Steiner (following a similar result by J. Sturm in 1823 for triangles) proved in 1825 that the area of pedal polygons of a polygon W with respect to points on any given circumference centered on K [33] is invariant.

range	invariant group	total
$k_{101}-k_{121}$	Distances, area, angles, curvature	21
$k_{201}-k_{205}$	N-Periodic Pedal polygons	5
$k_{301}-k_{307}$	Outer pedal polygon	7
$k_{401}-k_{407}$	Antipedal polygon	7
$k_{501}-k_{503}$	Steiner curvature centroid	3
$k_{601}-k_{610}$	Pairs of pedal polygons wrt. foci	8
$k_{701}-k_{703}$	Evolute polygons	3
$k_{801}-k_{818}$	Inversive objects	18
$k_{901}-k_{908}$	Pairs of Inversive objects	8
total:		82

TABLE 1. Numbering scheme for the invariants currently listed in this article.

On the invariant tables below, column “invariant” provides an expression for the conserved quantity; column “value” provides a closed-form expression for the invariant (when available) in terms of the fundamental constants, or a ‘?’ when not available (note that the invariant may already have been proved but no closed-form expression has yet been found); column “which N” specifies whether the invariant only holds for certain N (even, odd, etc.); column “date” specifies the month and year (mm/yy) when the invariant was first experimentally detected. Column “proven” references available proofs if already communicated and/or published, else it displays a ‘?’.

3.1. Basic Invariants. Invariants involving angles and areas of N-periodics and its tangential and internal polygons are shown on Table 2. There θ_i, A (resp. θ'_i, A') are angles, area of an N-periodic (resp. outer polygon to the N-periodic). A'' is the area of the internal polygon (where orbit touches caustic), see Figure 1. All sums/products go from $i = 1$ to N . $k_{101}, k_{102}, k_{103}$ originally studied in [26]. l_i and r_i denote $|P''_i - P_i|$ and $|P_{i+1} - P''_i|$, respectively and $d_{j,i} = |P_i - f_j|$. κ_i denotes the curvature of the EB at P_i (3). $\alpha_{j,i}$ denotes the angle $P_i f_j P_{i+1}$.

3.2. Pedal Polygons. Tables 3 and 4 describe invariants found for the *pedal polygons* of N-periodics and the outer polygon, see Figure 2.

3.3. Pedals with respect to N-periodic. Let Q_i be the feet of perpendiculars dropped from a point M onto the sides of the N -periodic. Let A_m denote the area of the polygon formed by the Q_i , Figure 2. Let ϕ_i denote the angle between two consecutive perpendiculars $Q_i - M$ and $Q_{i+1} - M$. Table 3 lists invariants so far observed for these quantities.

code	invariant	value	which N	date	proven
k_{101}	$\sum \cos \theta_i$	$JL - N$	all	4/19	[6, 9]
k_{102}	$\prod \cos \theta'_i$?	all	5/19	[6, 9]
k_{103}	A'/A	?	odd	8/19	[6, 11]
k_{104}	$\sum \cos(2\theta'_i)$?	all	1/20	[2]
k_{105}	$\prod \sin(\theta_i/2)$?	odd	1/20	[2]
k_{106}	$A'A$?	even	1/20	[11]
k_{107}	$k_{103}k_{105}$?	$\equiv 0 \pmod{4}$	1/20	?
k_{108}	k_{103}/k_{105}	?	$\equiv 2 \pmod{4}$	1/20	?
k_{109}	A/A''	k_{103}	odd	1/20	?
k_{110}	AA''	?	even	1/20	?
k_{111}	$A'A''$?	even	1/20	?
k_{112}	$A'A''/A^2$	1	odd	1/20	[3]
k_{113}	A'/A''	$[ab/(a''b'')]^2$	all	1/20	[32]
k_{114}	$\prod d_{1,i}$?	$\equiv 2 \pmod{4}$	4/20	?
k_{115}	$\prod P'_i - f_1 $?	$\equiv 0 \pmod{4}$	4/20	?
$*k_{116}$	$\prod l_i / \prod r_i$	1	all	5/20	[32]
$*k_{117}$	$\prod l_i, \prod r_i$?	even	5/20	?
$*k_{118}$	$\sum l_i, \sum r_i$	$L/2$	odd	8/20	?
$^\dagger k_{119}$	$\sum \kappa_i^{2/3}$	$L/[2J(ab)^{4/3}]$	all	10/20	[30]
$^\ddagger k_{120}$	$\sum \cos \alpha_{1,i}$?	all	10/20	?
k_{121}	$\sum d_{1,i}$?	even	10/20	symmetry

TABLE 2. Distance, area, and angle invariants displayed by the N-periodic, its outer and/or inner polygon. $*k_i, i = 116, 117, 118$ were discovered by Hellmuth Stachel. $^\dagger k_{119}$ was co-discovered with Pedro Roitman [27] and is equivalent to k_{902} . $^\ddagger k_{120}$ was suggested by A. Akopyan.

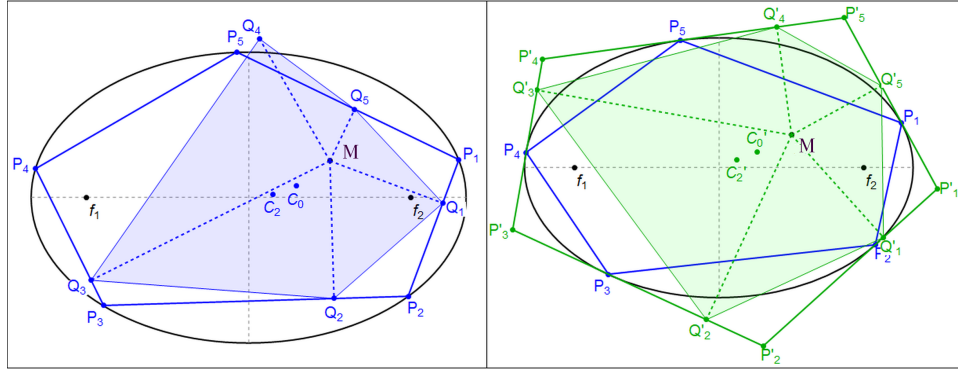


FIGURE 2. Left (resp. right): Pedal polygons for $N = 5$ from a point m with respect to the N-periodic (resp. its outer polygon). Vertex and area centroids C_0, C_2 are also shown. See Videos [24, PL#01,02,03].

code	invariant	value	which N	M	date	proven
${}^\dagger k_{201}$	$ Q_i - O $	a''	all	f_1, f_2	4/20	[4]
$k_{202,a}$	$\prod Q_i - M $	$(b'')^N$	even	f_1, f_2	4/20	[9]
$k_{202,b}$	$\prod Q_i - M $	$(a''b'')^{N/2}$	$\equiv 0 \pmod{4}$	O	4/20	[9]
$k_{203,a}$	$A A_m$?	$\equiv 0 \pmod{4}$	all	4/20	?
$k_{203,b}$	$A A_m$?	$\not\equiv 2 \pmod{4}$	O	4/20	?
k_{204}	A/A_m	?	$\equiv 2 \pmod{4}$	all	4/20	?
k_{205}	$\sum \cos \phi_i$?	all	all	4/20	[1]

TABLE 3. Invariants of pedal polygon with respect to N-Periodic sides. ${}^\dagger k_{201}$ means the locus of the vertices of a pedal with respect to a focus is a circle.

3.4. Pedals with respect to the Outer Polygon. Let Q'_i be the feet of perpendiculars dropped from a point M onto the outer polygon. Let ϕ'_i denote the angle between two consecutive perpendiculars $Q'_i - M$ and $Q'_{i+1} - M$. Let A'_m denote the area of the polygon formed by the Q'_i .

In the spirit of [29] we also analyze centers of mass: $C'_0 = \sum_i Q'_i / N$ is the vertex centroid, and the area centroid C'_2 of the polygon defined by the Q'_i (2). Table 4 lists invariants so far observed for these quantities.

code	invariant	value	which N	M	date	proven
${}^\dagger k_{301}$	$ Q'_i - O $	a	all	f_1, f_2	4/20	[4]
k_{302}	$\sum Q'_i - M ^2$?	all	all	4/20	[9]
$k_{303,a}$	$A' A'_m$?	$\equiv 2 \pmod{4}$	all	4/20	?
$k_{303,b}$	$A' A'_m$?	$\not\equiv 0 \pmod{4}$	O	4/20	?
k_{304}	A'/A'_m	?	$\equiv 0 \pmod{4}$	all	4/20	?
k_{305}	$\prod \cos \phi'_i$?	all	all	4/20	[1]
k_{306}	C'_0	?	all	all	4/20	[9]
k_{307}	C'_2	?	even	all	4/20	?

TABLE 4. Invariants of pedal polygon with respect to the sides of the outer polygon. ${}^\dagger k_{301}$ means the locus of the outer pedal with respect to a focus is a circle.

3.5. Antipedal Polygons. The antipedal polygons to the N -periodic and the outer polygon are shown in Figure 3. The antipedal polygon Q_i^* of P_i with respect to M is defined by the intersections of rays shot from every P_i along $(P_i - M)^\perp$.

Let A_m denote the area of the Q_i^* polygon and C_0^*, C_2^* its vertex- and signed ² area-centroids. $C_0'^*, C_2'^*$ refer to centers of antipedals of the outer polygon. Table 5 lists invariants found so far for these polygons.

3.6. Pedals of Steiner Curvature Centroids. Referring to Figure 4, let P, P', P'' denote as before the N -periodic, outer, and inner polygons, A, A', A'' their areas, and K, K', K'' their Steiner centroids of curvature (4). Let P_k, P'_k, P''_k denote the pedal polygons of P, P', P'' with respect to K, K', K'' , and A_k, A'_k, A''_k their areas.

²Antipedals can be self-intersecting.

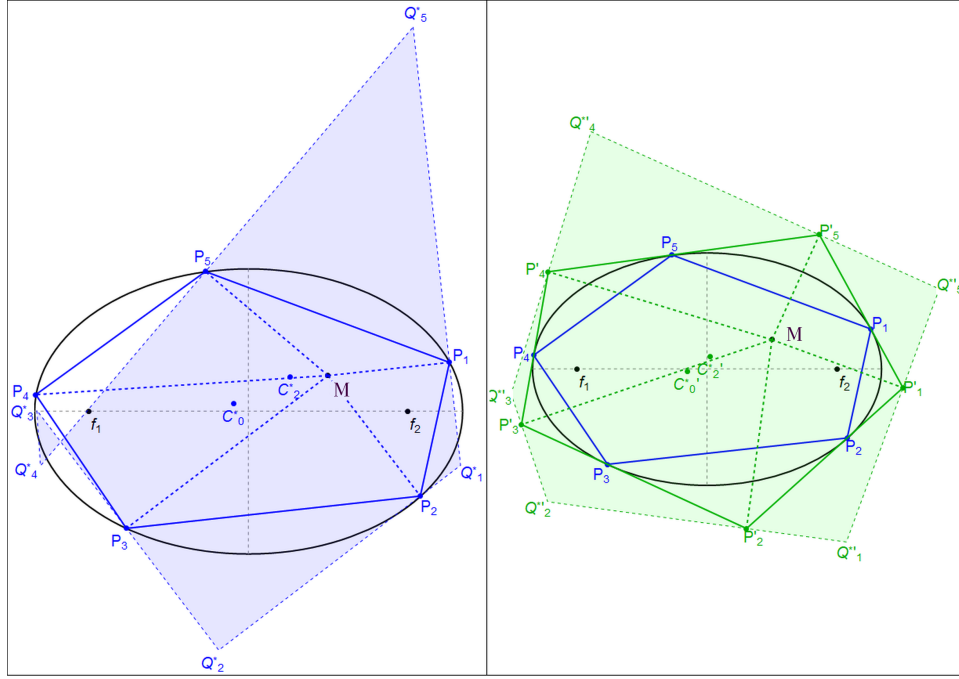


FIGURE 3. Left (resp. right): Antipedal polygons for $N = 5$ from a point m with respect to the N -periodic (resp. its outer polygon). Vertex and area centroids C_0^*, C_2^* are also shown.

code	invariant	value	which N	M	date	proven
k_{401}	$A' A_m^*$?	$\equiv 2 \pmod{4}$	all	4/20	?
k_{402}	A' / A_m^*	?	$\equiv 0 \pmod{4}$	all	4/20	?
$k_{403,a}$	$A_m A_m^*$?	odd	O	4/20	?
$k_{403,b}$	$A_m A_m^*$?	$\equiv 0 \pmod{4}$	f_1, f_2	4/20	?
k_{404}	A_m^* / A_m	?	$\equiv 2 \pmod{4}$	f_1, f_2	4/20	?
k_{405}	C_0^{*}	?	even	O, f_1, f_2	4/20	?
$k_{406,a}$	$C_0^{*'}, C_2^{*'}$	O	even	O	4/20	?
$k_{406,b}$	$C_0^{*'}, C_2^{*'}$?	4	f_1, f_2	4/20	?
k_{407}	$C_0^{*'}$?	even	f_1, f_2	4/20	?

TABLE 5. Invariants of antipedal polygons.

When N even, the curvature centroids are stationary at the origin, so invariants described before involving A, A_m (and primed quantities) for $M = O$ apply. For odd N , the Curvature Centroids move along individual ellipses concentric with the EB. Invariants are observed appear on Table 6.

Combining the above with k_{103} and k_{106} one obtains as corollaries the fact that A_k/A'_k , A_k/A''_k , and A'_k/A''_k are invariant for odd N .

3.7. Pairs of Focal Pedals and Antipedals. Let $\bar{Q}_{1,i}$ and $\bar{Q}_{2,i}$ be the vertices of the pedal polygon with respect to f_1 and f_2 . Define $q_{1,i} = |\bar{Q}_{1,i} - f_1|$ and

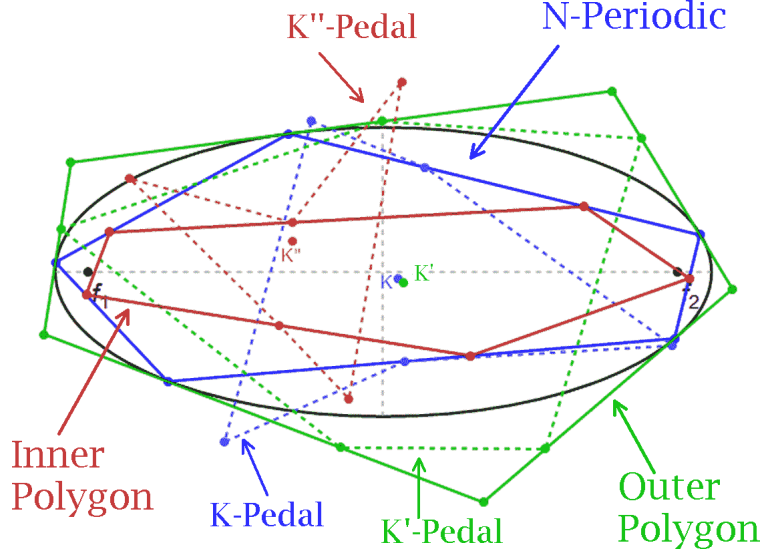


FIGURE 4. An N -periodic P is shown along with its outer P' and inner P'' polygons. Also shown are their Steiner centroids of curvature K, K', K'' and the the pedal polygons P_k, P'_k, P''_k with respect to said centroids.

code	invariant	value	which N	date	proven
k_{501}	A/A_k	?	odd	7/20	?
k_{502}	A'/A'_k	?	odd	7/20	?
k_{503}	A''/A''_k	?	odd	7/20	?

TABLE 6. Invariants of pedal polygons of N -periodic, outer, and inner polygons, with respect to their Steiner Curvature Centroids.

$q_{2,i} = |\bar{Q}_{2,i} - f_2|$. Likewise, let $\bar{Q}_{1,i}^*$ and $\bar{Q}_{2,i}^*$ be the vertices of the antipedal polygon with respect to f_1 and f_2 . Define $q_{1,i}^* = |\bar{Q}_{1,i}^* - f_1|$ and $q_{2,i}^* = |\bar{Q}_{2,i}^* - f_2|$.

Let \bar{A}_1 (resp. \bar{A}_2) denote the area of pedal polygon to N -periodics wrt f_1 (resp. f_2) onto the N -periodic, and similarly \bar{A}'_1, \bar{A}'_2 for the outer polygon focus-pedal. Table 7 list invariants so far detected involving pairs of these quantities.

Note $k_{604,a}, k_{604,b}$ can be proven via a symmetry argument, namely, area pair are equal since opposite vertices of an even N -periodic are reflections about the origin, as will be the pedal polygons from either focus.

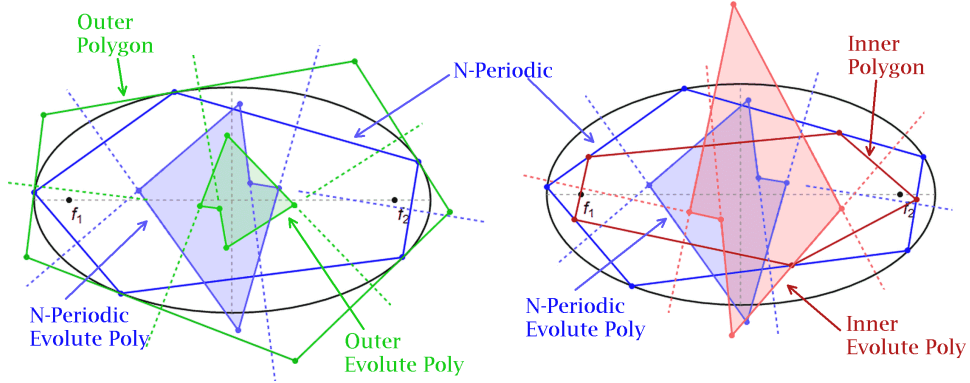
3.8. Evolute Polygons. After [8], let the evolute³ polygon R_{ev} of a generic polygon R have vertices at the intersections of successive pairs of perpendicular bisectors to the sides of R ; see Figure 5. So $P_{ev}, P'_{ev}, P''_{ev}$ denote the evolute polygons of $P, P',$ and P'' , respectively, and $A_{ev}, A'_{ev}, A''_{ev}$ their areas. Trivially, at $N = 3$ the latter vanish since perpendicular bisectors concur. At $N = 4$, P' is a rectangle, so $A'_{ev} = 0$. Area invariants observed for $N > 4$ appear on Table 8.

Combining the above with k_{103} and k_{106} one obtains as corollaries the fact that A_{ev}/A'_{ev} , A_{ev}/A''_{ev} , and A'_{ev}/A''_{ev} are invariant for all $N > 4$.

³The evolute of a smooth curve is the envelope of the normals [35, Evolute]. The perpendicular bisector is its discrete version.

code	invariant	value	which N	date	proven
k_{601}	$\sum q_{1,i} \sum q_{2,i}$?	odd	4/20	?
k_{602}	$\prod q_{1,i} \prod q_{2,i}$?	all	4/20	?
k_{603}	$\sum q_{1,i}^* / \sum q_{2,i}^*$	1	all	5/20	?
$k_{604,a}$	$\bar{A}_1 \cdot \bar{A}_2$?	odd	4/20	?
$k_{604,b}$	\bar{A}_1 / \bar{A}_2	1	even	4/20	symmetry
$k_{605,a}$	$\bar{A}'_1 \cdot \bar{A}'_2$?	odd	4/20	?
$k_{605,b}$	\bar{A}'_1 / \bar{A}'_2	1	even	4/20	symmetry
k_{606}	$\bar{A}_1 / \bar{A}_2 = \bar{A}'_1 / \bar{A}'_2$?	all	4/20	?
k_{607}	$\bar{A}_1^* / \bar{A}_2^*$	1	$\equiv 0 \pmod{4}$	10/20	?
k_{608}	$\bar{A}_1'^* / \bar{A}_2'^*$	1	even	10/20	?
k_{609}	$\bar{A}_1'' / \bar{A}_2''$	1	even	10/20	?
k_{610}	$\bar{A}_1''^* / \bar{A}_2''^*$	1	even	10/20	?

TABLE 7. Invariants between pairs of pedal polygons defined with respect to the foci.

FIGURE 5. **Left:** An N-Periodic and its outer polygon are shown along their evolute polygons whose vertices are ordered intersections of perpendicular bisectors. **Right:** N-periodic, inner polygon, and their evolute polygons.

code	invariant	value	which N	date	proven
k_{701}	A/A_{ev}	?	> 4	7/20	?
k_{702}	A'/A'_{ev}	?	> 4	7/20	?
k_{703}	A''/A''_{ev}	?	> 4	7/20	?

TABLE 8. Area-ratio invariants displayed by the evolute polygons of N-periodic, outer, and inner polygons.

3.9. Inversive Objects. Referring to Figure 6, let $P_{j,i}^{-1}$ denote the inversion of P_i , $i = 1, \dots, N$ with respect to a unit-radius circle centered on focus f_j , $j = 1, 2$, and $d_{j,i} = |P_i - f_j|$. Let \mathcal{P}_j^\dagger denote the polygon with vertices at $P_{j,i}^{-1}$. Let L_j^\dagger denote its perimeter, A_j^\dagger its area, and $\theta_{j,i}^\dagger$ its i th internal angle. Identical but primed symbols

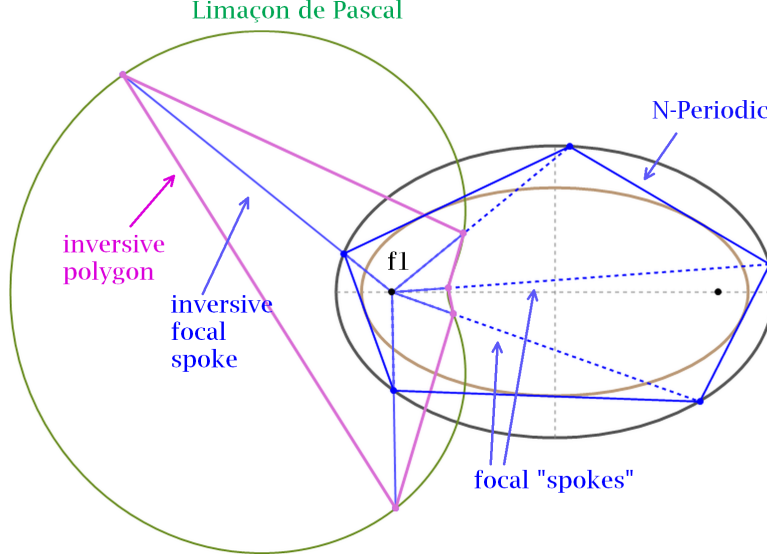


FIGURE 6. The vertices $P_{j,i}^{-1}$ of the inversive polygon \mathcal{P}_1 are obtained by inverting N-periodic vertices with respect to a unit-radius circle (not shown) centered on the left focus. The inversive focal spokes connect said focus to the vertices of \mathcal{P}_1 .

refer to the inversion of the outer polygon (vertices P'_i) with respect to f_j ; see Figure 7.

Let P_i^{\ominus} (resp. P_i^{\otimes}) denote the inversion of outer (resp. N-periodic) vertices with respect to the billiard (resp. caustic) ellipse. Recall the inversion of a point wrt to said ellipse is the midpoint of the chord joining the tangents from said point to said ellipse [17]. So the polygon \mathcal{P}'^{\otimes} (resp. \mathcal{P}^{\ominus}) defined by the P_i^{\ominus} (resp. P_i^{\otimes}) has vertices at the side midpoints of N-periodic (resp. inner polygon). Let their areas be denoted A^{\ominus} and A^{\otimes} , respectively.

Referring to Figure 8, let $A_{j,pol}$ and $A_{j,dual}$ denote the areas of the polar and dual polygons with respect to f_j , respectively. Let $\psi_{j,i}$ (resp. w_i) refers to the polar's i th angle (resp. dual's i th sidelength). Let $A_{j,ant}$ denote the area of the antipedal polygon wrt f_j , i.e., A_m^* for $M = f_j$. Recall that the dual is the inverse of the pedal [7], therefore the inversive and antipedal polygons are also inverses of each other. Let f'_1, f'_2 be the foci of the elliptic locus of the outer polygons' vertices (non-confocal though concentric and axis aligned with the billiard pair). Let P_j^{\ddagger} denote the inversion of the P'_i wrt f'_j and A_j^{\ddagger} denote the area of the polygon defined by the P_j^{\ddagger} .

Table 9 lists invariants of inversive objects defined with respect to a chosen focus (e.g. f_1), whereas Table 10 presents invariants involving a pair of inversive objects, defined with respect of both foci.

4. EXPERIMENTAL METHOD

A numeric/visualization toolbox was developed in Wolfram Mathematica [36] to accurately calculate and display N -periodics while reporting their areas, angles, etc., and those of some derived objects (pedal and inversive polygons, etc.); see Figure 9.

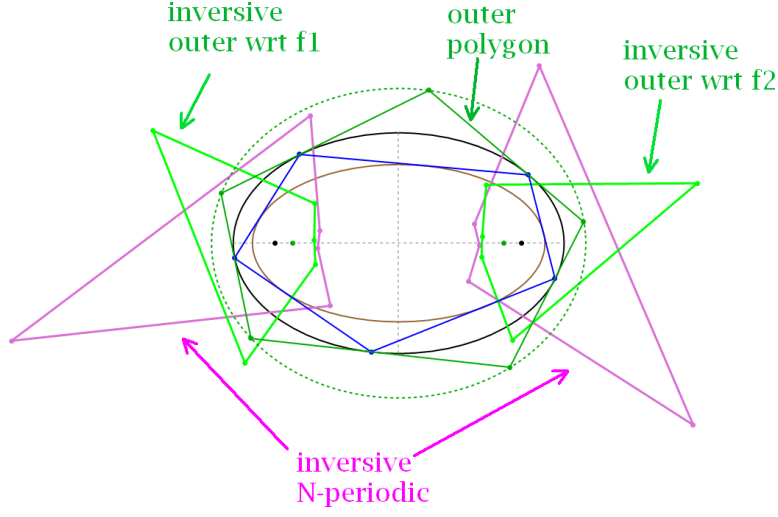


FIGURE 7. The pair of inversive orbit (resp. outer) polygons is obtaining by inverting the N-periodic (resp. outer polygon) with respect to a circle centered on each focus.

code	invariant	value	which N	date	proven
k_{801}	$\sum 1/d_{j,i}$?	all	10/20	[27, 6]
k_{802}	L_j^\dagger	?	all	10/20	?
$^{**}k_{803}$	$\sum \cos \theta_{j,i}^\dagger$?	$\neq 4$	10/20	?
$k_{804,a}$	$A A_j^\dagger$?	$\equiv 0 \pmod{4}$	10/20	?
$k_{804,b}$	$A A_j^\dagger$	4	4	10/20	?
k_{805}	A/A_j^\dagger	?	$\equiv 2 \pmod{4}$	10/20	?
$k_{806,a}$	$A_j'^\dagger/A_j^\dagger$?	all	10/20	?
$k_{806,b}$	$A_j'^\dagger/A_j^\dagger$	2	4	10/20	?
$^\dagger k_{807}$	$A.A^\otimes$?	even	10/20	?
k_{808}	A/A^\otimes	?	odd	10/20	?
$^\dagger k_{809}$	$A'.A'^\ominus$?	even	10/20	?
k_{810}	A'/A'^\ominus	?	odd	10/20	?
$^\ddagger k_{811}$	$\sum w_i^2$?	all	10/20	?
$k_{812,a}$	$\sum \cos \psi_{1,i}$?	all	10/20	?
$k_{812,b}$	$\sum \cos \psi_{1,i}$	0	4	10/20	?
k_{813}	$A_{j,pol}/A_{j,inv}$?	all	10/20	?
k_{814}	$A_{j,pol}/A_{j,dual}$?	all	10/20	?
k_{815}	$A_{j,ped}^\dagger \cdot A_{j,dual}$?	odd	10/20	?
k_{816}	$A_{j,ped}^\dagger/A_{j,dual}$?	even	10/20	?
k_{817}	$A_{j,ped}^\dagger \cdot A_{j,ant}$?	$\equiv 0 \pmod{4}$	10/20	?
k_{818}	$A_{j,ped}^\dagger/A_{j,ant}$?	$\equiv 2 \pmod{4}$	10/20	?

TABLE 9. Invariants of inversive objects over the N-periodic family. $^{**}k_{803}$ Co-discovered with Pedro Roitman [27]. $^\dagger k_{807-810}$ The inverted vertices P_i^\otimes (resp. $P_i'^\ominus$) are at the midpoints of the inner (resp. N-periodic orbit) segments. $^\ddagger k_{814}$ Discovered by A. Akopyan [5].

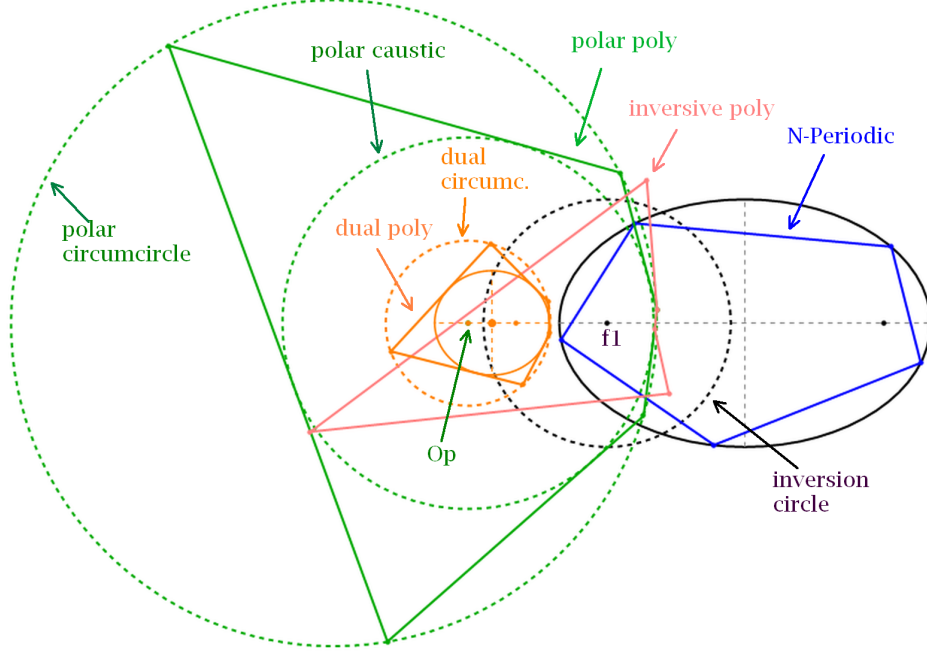


FIGURE 8. Polygons derived from N-periodics: (i) inversive: vertices are inversions of the P_i wrt to a unit circle centered on a focus, e.g., f_1 ; (ii) polar: antipedal of the inversive wrt to f_1 . The locus of its vertices is a circle non-concentric with an also circular caustic. Let O_p denote the latter's center. (iii) dual: inversion of the polar with respect to O_p . This produces a Poncelet family inscribed in a circle centered on O_p and circumscribed about an ellipse with one focus on O_p .

code	invariant	value	which N	date	proven
k_{901}	$\sum d_{1,i}^{-1} / \sum d_{2,i}^{-1}$	1	all	10/20	from k_{801}
$*k_{902}$	$\sum 1/(d_{1,i} d_{2,i})$	$L/[2J(ab)^2]$	all	10/20	[30]
$k_{903,a}$	$A_1^\dagger \cdot A_2^\dagger$?	odd	10/20	?
$k_{903,b}$	$A_1^\dagger / A_2^\dagger$	1	even	10/20	symmetry
$k_{904,a}$	$A_1^{\prime\dagger} \cdot A_2^{\prime\dagger}$?	odd	10/20	?
$k_{904,b}$	$A_1^{\prime\dagger} / A_2^{\prime\dagger}$	1	even	10/20	symmetry
k_{905}	$A_1^{\prime\prime\dagger} / A_2^{\prime\prime\dagger}$	1	even	10/20	?
k_{906}	$A_1^{\prime\dagger} / A_2^{\prime\dagger}$	1	even	10/20	?
$k_{907,a}$	$A_{1,dual}^\dagger \cdot A_{2,dual}^\dagger$?	odd	10/20	?
$k_{907,b}$	$A_{1,dual}^\dagger / A_{2,dual}^\dagger$	1	even	10/20	?
$k_{908,a}$	$A_{1,ped}^\dagger / A_{2,ped}^\dagger$	1	even	10/20	?
$k_{908,b}$	$A_{1,ped}^\dagger \cdot A_{2,ped}^\dagger$	1	3	10/20	?

TABLE 10. Invariants of pairs of inversive objects defined with respect to the foci f_1, f_2 . As observed by A. Akopyan, $*k_{902}$ is in fact equivalent to k_{119} , see (3).

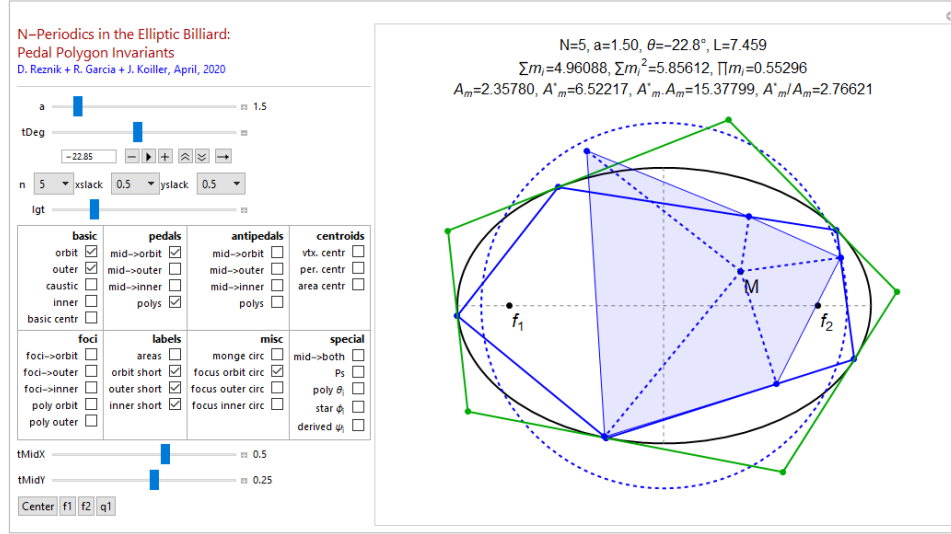


FIGURE 9. Interactive toolbox written in Wolfram Mathematica [36]. The area on the left permits selection of specific geometries, whereas on the right, the EB, the N-Periodic and derived polygons is displayed. See Videos on Table 11.

Since all trajectories in the Billiard family are tangent to the same confocal caustic, a crucial calculation is to obtain one caustic semiaxis, e.g., a'' for a given choice of a, b , and N . We achieve this for all N via non-linear least-squares minimization [20] of the bisection error. Namely:

- Initialize N vertices P_i evenly across the ellipse (pick $t_i, i = 1, \dots, N$ for each), and let $P_1 = (a, 0)$.
- Let b_i be the unit bisector of the N -gon sides incident at P_i . Let n_i denote the ellipse normal at the P_i . The P_i will be a legitimate closed billiard trajectory if all bisectors are perfectly aligned with the local normals, i.e., if P_i^* can be found which make the following error vanish:

$$\mathcal{E} = \sum_{i=1}^N (n_i^T \cdot b_i)^2$$

- Obtain the unique confocal ellipse tangent to $[a, 0]P_2^*$.

Notice only $N/2$ vertices for N odd (resp. $N/4$ for N even) need to be optimized if one exploits the symmetries of odd (resp. even) vertex positions when $P_1 = (a, 0)$.

In terms of identifying invariants, we look for quantities which over hundreds of configurations of a given N -family are statistically constant, maintained over a range of Billiard aspect ratios.

5. VIDEO LIST

Videos of some of the above phenomena have been placed on a Youtube [playlist](#) [25] and are listed individually on Table 11.

Id	Title	N	youtu.be/...
01	Area Invariants of Pedal and Antipedal Polygons	3	LN623VjeeFQ
02	Exploring invariants of N-Periodics and pedal polygons	3–12	2yXb0V7qf7k
03	Centroid Stationarity of Pedal Polygons	even	j_GD_g8aIbg
04	Equal sum of distances from foci to vertices of Antipedal Polygon	3–6	6F7Y3UKJzdk
05	Concyclic feet of focal pedals and product of sums of lengths for odd N	5,6	0T-xAdb0p8o
06	Invariant altitudes of N-Periodics and outer polygons I	3,4	MvZhWbI6iB8
07	Invariant altitudes of N-Periodics and outer polygon II	5,6	ZMHLmwXeKrM
08	Sum of focal squared altitudes to outer polygon	3–8	VUtBRzmb0YU
09	Sum of square altitudes from arbitrary point to outer polygon	5	RNmHROZNGj8
10	Area products of focal pedal polygons	5	sw8pJFMV00w
11	Area ratios of Pedal Polygons to N-Periodic and outer Polygon	5,6	6F7Y3UKJzdk
12	Invariant Area Ratios to Minimum-Area Steiner Pedal Polygons	5	f0JwRlu7iaY
13	N-Periodic Inversive Invariants	5	wkstGKq5j0o
14	N-Periodic Inversive Objects	5	bFsehsbizls
15	Odd N-Periodics in the Elliptic Billiard: Invariant Area Product of Focus-Inversive Polygons	5	bTkbdEPNUOY
16	Invariants of Inversive, Polar, and Dual Polygons derived from Billiard N-Periodics	5	qyAHOW32NXY
17	Centers of N-Periodic Inversive Arcs: Bicentric Poncelet Family w/ Invariants	5	mXkk_4RYrnU
18	$N = 6$, $a/b = 2$ antipedal polygon has zero signed area	5	f0AES-CzjNI

TABLE 11. Youtube list of videos about invariants of N-Periodics, the last column provides the link.

ACKNOWLEDGMENTS

We would like to thank Olga Romaskevitch, Sergei Tabachnikov, Richard Schwartz, Arseniy Akopyan, Hellmuth Stachel, Alexey Glutsyuk, Corentin Fierobe, Maxim Arnold, and Pedro Roitman for useful discussions and insights.

The second author is fellow of CNPq and coordinator of Project PRONEX/CNPq/FAPEG 2017 10 26 7000 508.

APPENDIX A. TABLE OF SYMBOLS

symbol	meaning
O, f_1, f_2, N	center and foci of billiard
$(a, b), (a'', b'')$	billiard (resp. caustic) major, minor semi-axes
N, L, J	trajectory sides, inv. perimeter and Joachimsthal's constant
P_i, P'_i, P''_i	N -periodic, outer, inner polygon vertices
$d_{j,i}, l_i, r_i$	distances $ P_i - f_j , P''_i - P_i , P_{i+1} - P''_i $
$\theta_i, \theta'_i, \alpha_{j,i}$	N -periodic, outer poly, and $P_i f_j P_{i+1}$ angles
A, A', A''	N -periodic, outer, inner areas
M	a point in the plane of the billiard
Q_i, Q'_i, Q''_i	vertices of the pedal polygon of N -periodic, outer, inner polygon wrt M
$Q_i^*, Q_i^{*'}, Q_i^{*''}$	vertices of the antipedal polygon of the N -periodic, outer, inner polygon wrt M
$\phi_i, \phi'_i, \phi''_i$	ith angle of pedal polygon of N -periodic, outer, inner polygons wrt M
A_m, A'_m, A_m^*	areas of Q_i, Q'_i, Q_i^* polygons
C_0, C'_0, C_0^*	vertex centroids of the Q_i, Q'_i, Q_i^* polygons
C_2, C'_2, C_2^*	area centroids of the Q_i, Q'_i, Q_i^* polygons
$C_0^{*'}, C_2^{*'}$	vertex, area centroids of the $Q_i^{*'}$ polygon
$\bar{Q}_{j,i}, \bar{Q}_{j,i}^*$	vertices of N -periodic pedal, antipedal polygon wrt. f_j
$q_{j,i}, q_{j,i}^*$	$ \bar{Q}_{j,i} - f_j $ and $ \bar{Q}_{j,i}^* - f_j $
\bar{A}_j, \bar{A}_j^*	areas of $\bar{Q}_{j,i}$ and $\bar{Q}_{j,i}^*$ polygons
K, K', K''	Steiner centroids of curvature of P, P', P''
P_k, P'_k, P''_k	Pedal Polygons of P, P', P'' wrt. K, K', K''
A_k, A'_k, A''_k	Areas of P_k, P'_k, P''_k
$P_{ev}, P'_{ev}, P''_{ev}$	Evolute Polygons of P, P', P''
$A_{ev}, A'_{ev}, A''_{ev}$	Areas of $P_{ev}, P'_{ev}, P''_{ev}$
$P_{j,i}^{-1}$	inversion of P_i wrt. to unit-radius circle centered on f_j
$\mathcal{P}_j^\dagger, L_j^\dagger, A_j^\dagger$	polygon defined by $P_{j,i}^{-1}$, its perimeter, and area
$\theta_{j,i}^\dagger$	internal angle of \mathcal{P}_j^\dagger at $P_{j,i}^{-1}$
f'_1, f'_2	foci of the elliptic locus of the P'_i
$P_j^{\dagger\ddagger}, A_j^{\dagger\ddagger}$	inversion of P'_i wrt to f'_j , area of $P_j^{\dagger\ddagger}$ poly
$\mathcal{P}^\otimes, \mathcal{P}'^\ominus$	inversion of P_i (resp. P'_i) wrt caustic (resp. billiard)
A^\otimes, A'^\ominus	areas of $\mathcal{P}^\otimes, \mathcal{P}'^\ominus$
$\psi_{j,i}, w_i$	ith angle of polar (sidelength of dual) polygon wrt f_j
$A_{j,pol}, A_{j,dual}$	area of polar, dual polygon wrt f_j
$A_{j,ped}, A_{j,ant}$	area of pedal, antipedal polygon wrt f_j

TABLE 12. Symbols used in the invariants. Note $i = 1, \dots, N$ and $j = 1, 2$. Note any single (resp. double) primed quantities apply to the outer (resp. inner) polygons.

REFERENCES

- [1] Akopyan, A. (2020). Angles $\phi = \pi - \theta_i$ (resp. $\phi' = \phi - \theta'_i$), so equivalent to invariant sum (resp. product) of cosines. Private Communication.
- [2] Akopyan, A. (2020). Corollary of Theorem 6 in Akopyan et al., “Billiards in Ellipses Revisited” (2020). Private Communication.
- [3] Akopyan, A. (2020). Follows from previous results: the construction is affine and holds for any two concentric conics. Private Communication.
- [4] Akopyan, A. (2020). Perpendicular feet to N-periodic or its tangential polygon are cyclic. Private Communication.
- [5] Akopyan, A. (2020). Sum of squared sidelengths of focus-polar polygon is invariant. Private Communication.
- [6] Akopyan, A., Schwartz, R., Tabachnikov, S. (2020). Billiards in ellipses revisited. *Eur. J. Math.* doi.org/10.1007/s40879-020-00426-9.
- [7] Akopyan, A., Zaslavski, A. (2007). *Geometry of Conics*. Mathematical world. Providence: American Mathematical Society.
- [8] Arnold, M., Fuchs, D., Izmistiev, I., Tabachnikov, S., Tsukerman, E. (2017). Iterating evolutes and involutes. *Discrete Comput. Geom.*, 58: 80–143. doi.org/10.1007/s00454-017-9890-y.
- [9] Bialy, M., Tabachnikov, S. (2020). Dan Reznik’s identities and more. *Eur. J. Math.* doi.org/10.1007/s40879-020-00428-7.
- [10] Chang, S.-J., Friedberg, R. (1988). Elliptical billiards and Poncelet’s theorem. *J. Math. Phys.*, 29: 1537–1550.
- [11] Chavez-Caliz, A. (2020). More about areas and centers of Poncelet polygons. *Arnold Math J.* doi.org/10.1007/s40598-020-00154-8.
- [12] Dragović, V., Radnović, M. (2011). *Poncelet Porisms and Beyond: Integrable Billiards, Hyperelliptic Jacobians and Pencils of Quadrics*. Frontiers in Mathematics. Basel: Springer.
- [13] Dragović, V., Radnović, M. (2014). Bicentennial of the great Poncelet theorem (1813–2013): current advances. *Bulletin Amer. Math. Soc.*, 51(3): 373–445.
- [14] Dragović, V., Radnović, M. (2006). A survey of the analytical description of periodic elliptical billiard trajectories. *J. of Math. Sci.*, 135: 3244–3255. doi.org/10.1007/s10958-006-0154-2.
- [15] Garcia, R., Reznik, D. (2020). Explicit expressions for some elliptic billiard invariants. In preparation.
- [16] Garcia, R., Reznik, D., Koiller, J. (2020). New properties of triangular orbits in elliptic billiards. *Amer. Math. Monthly*, to appear.
- [17] Glaeser, G., Stachel, H., Odehnal, B. (2016). *The Universe of Conics: From the ancient Greeks to 21st century developments*. Berlin: Springer.
- [18] Izmistiev, I., Tabachnikov, S. (2017). Ivory’s theorem revisited. *Journal of Integrable Systems*, 2. doi.org/10.1093/integr/xyx006.
- [19] Kaloshin, V., Sorrentino, A. (2018). On the integrability of Birkhoff billiards. *Phil. Trans. R. Soc.*, A(376).
- [20] Nocedal, J., Wright, S. (2006). *Numerical Optimization*, chap. 10. New York: Springer, 2nd ed., pp. 245–269. Least-Squares Problems.
- [21] Nomizu, K., Sasaki, T. (1994). *Affine Differential Geometry*. Cambridge: Cambridge University Press.
- [22] Preparata, F., Shamos, M. (1988). *Computational Geometry - An Introduction*. New York: Springer-Verlag, 2nd ed.
- [23] Ramírez-Ros, R. (2014). On Cayley conditions for billiards inside ellipsoids. *Nonlinearity*, 27(5): 1003–1028.
- [24] Reznik, D. (2020). Playlist for “Invariants of 3- and 4-Periodics in the Elliptic Billiard”. YouTube. bit.ly/3aNgqgU.
- [25] Reznik, D. (2020). Playlist for “Invariants of N-Periodics in the Elliptic Billiard”. YouTube. bit.ly/2xeVGyW.
- [26] Reznik, D., Garcia, R., Koiller, J. (2020). Can the elliptic billiard still surprise us? *Math. Intelligencer*, 42: 6–17. rdcu.be/b2cg1.
- [27] Roitman, P. (2020). Investigation of n-periodic invariants involving the curvature of the ellipse. Private Communication.
- [28] Rozikov, U. A. (2018). *An Introduction To Mathematical Billiards*. Singapore: World Scientific Publishing Company.

- [29] Schwartz, R., Tabachnikov, S. (2016). Centers of mass of Poncelet polygons, 200 years after. *Math. Intelligencer*, 38(2): 29–34. doi.org/10.1007/s00283-016-9622-9.
- [30] Stachel, H. (2020). Closed form expression for k_{119} . Private Communication.
- [31] Stachel, H. (2020). Joachimsthal's constant in terms of a , b and a'' . Private Communication.
- [32] Stachel, H. (2020). Proofs for k_{113} and k_{116} . Private Communication.
- [33] Steiner, J. (1838). Über den Krümmungs-Schwerpunkt ebener Curven. *Abhandlungen der Königlichten Akademie der Wissenschaften zu Berlin*: 19–91.
- [34] Tabachnikov, S. (2005). *Geometry and Billiards*, vol. 30 of *Student Mathematical Library*. Providence, RI: American Mathematical Society. bit.ly/2RV04CK.
- [35] Weisstein, E. (2019). Mathworld. mathworld.wolfram.com.
- [36] Wolfram, S. (2019). Mathematica, version 10.0.

DATA SCIENCE CONSULTING, RIO DE JANEIRO, BRAZIL
 Email address: dreznik@gmail.com

MATH & STATISTICS INSTITUTE, FEDERAL UNIVERSITY OF GOIÁS, GOIÂNIA, BRAZIL
 Email address: ragarcia@ufg.br

FEDERAL UNIVERSITY OF RIO DE JANEIRO, RIO DE JANEIRO, BRAZIL
 Email address: jairkoiller@gmail.com